Fault-tolerant architecture for quantum computation using electrically controlled semiconductor spins

J. M. TAYLOR[1]*, H.-A. ENGEL[1], W. DÜR[2], A. YACOBY[3], C. M. MARCUS[1], P. ZOLLER[2] AND M. D. LUKIN[1]

[1]Department of Physics, Harvard University, Cambridge, Massachusetts 02138, USA

[2]Institute for Theoretical Physics, University of Innsbruck, and Institute for Quantum Optics and Quantum Information of the Austrian Academy of Sciences, A-6020 Innsbruck, Austria

[3]Department of Condensed Matter Physics, Weizmann Institute of Science, Rehovot 76100, Israel

*e-mail: taylor@physics.harvard.edu

Published online: 1 December 2005; doi:10.1038/nphys174

Information processing using quantum systems provides new paradigms for computation and communication and may yield insights into our understanding of the limits of quantum mechanics. However, realistic systems are never perfectly isolated from their environment, hence all quantum operations are subject to errors. Realization of a physical system for processing of quantum information that is tolerant of errors is a fundamental problem in quantum science and engineering. Here, we develop an architecture for quantum computation using electrically controlled semiconductor spins by extending the Loss–DiVincenzo scheme and by combining actively protected quantum memory and long-distance coupling mechanisms. Our approach is based on a demonstrated encoding of qubits in long-lived two-electron states, which immunizes qubits against the dominant error from hyperfine interactions. We develop a universal set of quantum gates compatible with active error suppression for these encoded qubits and an effective long-range interaction between the qubits by controlled electron transport. This approach yields a scalable architecture with favourable error thresholds for fault-tolerant operation, consistent with present experimental parameters.

Significant effort has been directed towards the physical realization of quantum computation. The promise of solid-state systems such as quantum dots[1] and superconducting islands[2,3] was identified early on. Coherent manipulation of solid-state quantum bits, analogous to well-developed realizations in atomic physics[4,5], has been experimentally demonstrated[6–9]. However, achieving fault-tolerant quantum computation entails a significant mitigation of environmental couplings, which is particularly challenging in the solid state. Here, we develop a scalable architecture for solid-state quantum computation based on actively protected two-electron spin states in quantum dots[10–17]. We find a universal set of gates for these encoded states that can be implemented using only local electrical control and that suppress the effect of hyperfine interactions, the dominant source of error[9,18–23]. Our architecture allows for a modular, hierarchical design and includes autonomous control and non-local coupling by means of controlled electron transport. Fault-tolerant operation[24] seems to be achievable with present experimental methods.

As demonstrated experimentally[9], exchange interactions can be used to prepare qubits in well-defined states, protect them from low-frequency noise[14,17], perform certain single-qubit rotations[15,16] and allow measurement by means of charge readout with a nearby electrometer[25–27]. Control of the exchange energy J between adjacent quantum dots is achieved by electrical means. We expand these operations to include single-qubit rotations based on waiting in small static magnetic-field gradients, and two-qubit gates based on the capacitive interaction of four electrons in proximal double dots, completing the universal set of quantum gates compatible with dynamical protection and electrical control. Effective long-range coupling between qubits is provided by moving electrons using a single-electron pump or charge-coupled device[28], which allow for many electrons to be transported in parallel before and after two-qubit operations, such that they are immune to most dephasing processes during transport[17]. Together, these elements allow us to develop a fully electrical architecture for controlling

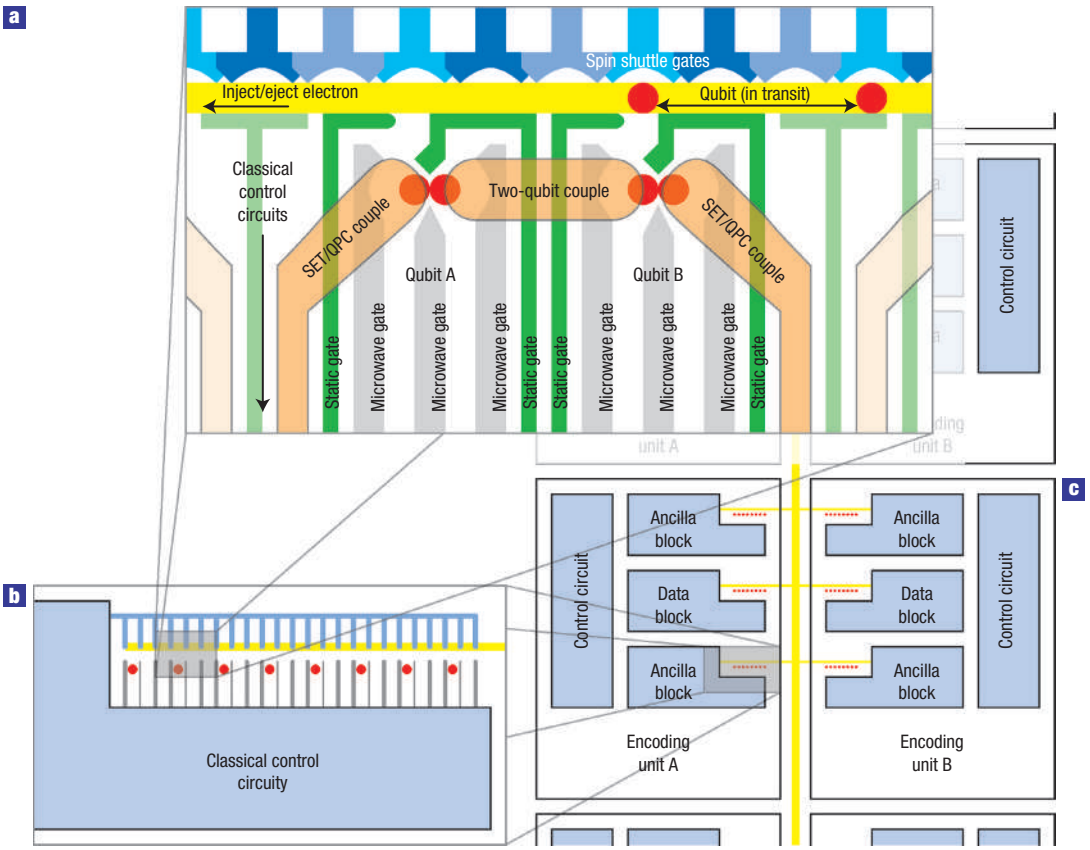

Figure 1 Architecture for quantum computation. a, Two adjacent depletion-gate-defined double quantum dots (one qubit comprising two spins) built on a semiconductor heterostructure, with tuning gates (green), high-frequency microwave gates (grey, blue) and capacitive coupling gates (orange) forms a node. Coupling to a nearby quantum point contact (QPC) or single-electron transistor (SET) provides for charge measurement. Alternating gates along the top form the spin shuttle and a Fermi sea can be selectively coupled to the spin shuttle for electron injection/ejection (preparation and erasure). The transport-channel double dot (qubit B) is only occupied during two-qubit gates. **b**, Qubits (red) connected by a spin shuttle (yellow), along with semi-autonomous classical control circuitry (blue–grey), forming a single block. **c**, A single 'data' block, used for the logical computation, is adjacent to *R* ancilla blocks, making up an 'encoding unit'. Ancilla blocks may operate in parallel; as soon as a verified ancilla is available, it may be used for error correction within the unit. Encoding units, in turn, operate autonomously, allowing for the massive parallelism necessary for large-scale error correction. Replacing the two-qubit 'node' of **a** with two encoding units in **c** allows for recursive implementation of QEC codes; such code concatenation improves the error-correcting abilities of the system, eventually allowing for arbitrary computations as long as physical error rates are less than some threshold values.

and coupling qubits (Fig. 1) that is highly modular and designed for efficient quantum error correction (QEC). By analogy with scalable ion-trap schemes[14,29,30], we find a better fault-tolerant error threshold than nearest-neighbour architectures[31].

PROTECTED QUBITS AND QUANTUM GATES

The present approach takes singlet and triplet states of two electron spins in adjacent quantum dots[32] to encode one qubit (Figs 1a and 2a). The logical basis of our qubits is defined by $|0_L\rangle = (|\uparrow\downarrow\rangle - |\downarrow\uparrow\rangle)/\sqrt{2}$ and $|1_L\rangle = (|\uparrow\downarrow\rangle + |\downarrow\uparrow\rangle)/\sqrt{2}$. This decoherence-free subspace immediately protects the system from collective phase noise due, for example, to uniform magnetic-field fluctuations[10–12]. In addition, dynamical protection from differential phase noise, due, for example, to hyperfine interaction with nuclear spins[17], is possible within this subspace[13] by means of periodic exchange (SWAP) of the two electrons[9,14]. An external magnetic field produces an energy gap between the unused states $|\uparrow\uparrow\rangle, |\downarrow\downarrow\rangle$ and the logical subspace, thereby suppressing spin-flip errors[18,33,34]. With these protections, a quantum memory with decoherence times approaching milliseconds may be achieved[17].

We model each double dot (Fig. 2a) as a three-level system (Fig. 2b): the two logical states $|0_L\rangle, |1_L\rangle$ and the state $|(0,2)S\rangle$, used for preparation, for measurement and for quantum gate operations, respectively. The logical states have one electron in each well, a charge configuration labelled (1,1), whereas the state $|(0,2)S\rangle$ is a spin singlet of the biased system with two electrons in a single dot and no electrons in the other, a charge configuration labelled (0,2). Its energy detuning Δ from the logical subspace and its tunnelling couple T to the singlet $|0_L\rangle$ are controlled by local electric gates. When detuning is large and negative ($\Delta \ll -T$), $|(0,2)S\rangle$ is the ground state of the system. For $\Delta \gg T$, the state $|(0,2)S\rangle$ is only virtually populated, which leads to an effective exchange energy $J \sim T^2/\Delta$ (see Methods); in terms of practical parameters, J may be 0–100 μeV. Rapid control of the exchange energy may be accomplished through control of any combination of T and Δ. To complete the set of single qubit operations, we require a static magnetic-field gradient dB between two dots. It mixes states within the logical subspace, acting as a qubit-flip term. This gradient could be produced by steady-state nuclear polarizations, Landé g-factor differences or permanent magnets. Polarizations of ∼0.5% or a dot-to-dot difference in g-factor of 1% at 3 T of external field gives a

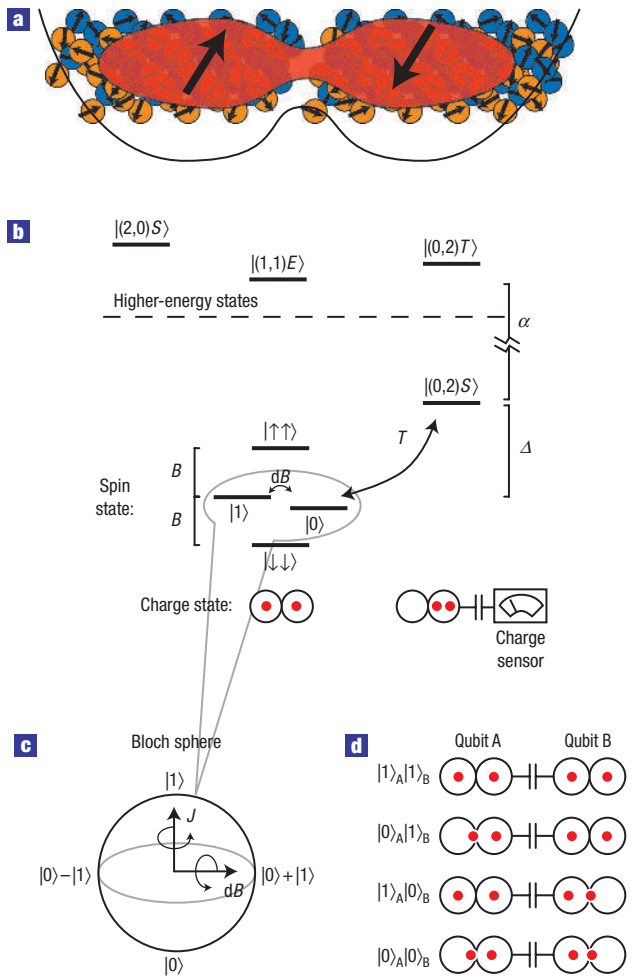

Figure 2 Logical qubit. a, Schematic of a double quantum dot, with two-electron spins (red) confined in a double-well potential (black line) and interacting with lattice nuclei (orange and blue). **b**, Level diagram, indicating logical states coupled by magnetic-field gradient, further coupling of the (0,2) charge state $|(0,2)S\rangle$ to the singlet ($|0_L\rangle$) and the 'leakage' states, $|\uparrow\uparrow\rangle, |\downarrow\downarrow\rangle$. The triplets of the biased system are neglected owing to a large exchange energy $J_d \approx \alpha$ and the spin-aligned triplets with one electron in each well ($|\uparrow\uparrow\rangle, |\downarrow\downarrow\rangle$) are detuned by Zeeman energy. Higher-energy states such as the excited state $|(1,1)E\rangle$, separated by an orbital-level spacing $\alpha \approx 0.5$–1 meV, may be included as further renormalization corrections. **c**, The Bloch sphere of the logical space, with rotation axes due to exchange interactions, J, and gradient field terms, dB. **d**, Truth table for interaction between two adjacent double dots (schematically shown as coupled quantum double dots), used for the two-qubit CPHASE gate as described in the text.

30 mT gradient between dots; similarly, nearby permanent magnets can product gradients upwards of 100 mT μm^{-1} (ref. 35).

For a universal set of gates we choose rotations around the Z ($|0_L\rangle, |1_L\rangle$) and X ($|\uparrow\downarrow\rangle, |\downarrow\uparrow\rangle$) axes of the effective Bloch sphere shown in Fig. 2c, and a controlled-phase two-qubit gate. Preparation, measurement and Z rotations within the logical space have already been demonstrated experimentally[9]. In brief, the state $|0_L\rangle$ can be prepared by loading two electrons from a nearby Fermi sea into the ground state of a single quantum dot, $|(0,2)S\rangle$ when $\Delta < 0$. The two electrons are then split by changing the detuning Δ from large and negative to large and positive, fast with respect to the gradient energy $\epsilon_{dB} = 2g^*\mu_B dB$ but adiabatic with respect to T, yielding adiabatic passage of $|(0,2)S\rangle$ to $|0_L\rangle$. Here g^* is the effective g-factor of the electron and μ_B is the Bohr magneton. The reversed process adiabatically transfers the singlet state ($|0_L\rangle$) to $|(0,2)S\rangle$; this state differs in charge from $|1_L\rangle$, which still has one electron in each dot, thereby allowing for measurement of the logical states by means of charge measurement. As illustrated in Fig. 2c, exchange interaction[1,15], with $J \neq 0$ for a time $t = \hbar\phi/J$, yields a Z-axis rotation of angle ϕ: $R_Z^\phi = e^{-i\phi\sigma_z/2}$, where $\sigma_{x,y,z}$ are the Pauli matrices within the logical subspace and $\hbar = 1.05457 \times 10^{-34}$ J s. Similarly, the gradient, dB, produces logical X rotations; by waiting with $J = 0$ for a time $t = \hbar\phi/\epsilon_{dB}$, an X rotation $R_X^\phi = e^{-i\phi\sigma_x/2}$ is obtained. In the regime of large J and relatively small gradients dB, an arbitrary rotation is created by choosing the timing of Z rotations such that the desired X rotation is accomplished during free evolution (when $J = 0$). Undesired X rotations, such as those accumulated during waiting intervals, are removed by the SWAP operation used to refocus the system for protection against nuclear spins. Alternative approaches for the regime of large dB and small J are possible by working in the rotating frame of the gradient and oscillating J at a frequency commensurate with the energy difference, ϵ_{dB} (ref. 15).

Coulomb interaction between two double dots (qubits A and B in Fig. 2d) is used for two-qubit gates. It is described by the hamiltonian $V_{AB} = E_{cc}|(0,2)S\rangle\langle(0,2)S|_A \otimes |(0,2)S\rangle\langle(0,2)S|_B$ where E_{cc} is the differential cross-capacitance energy between the two double-dot systems, corresponding to the difference in Coulomb energy from the (0,2)–(0,2) configuration and the (1,1)–(1,1) configuration. Simultaneously reducing the detuning of two nearby qubits (A and B) makes the states $|0_L\rangle_{A,B}$ adiabatically transfer to a state that has an admixture of $|(0,2)S\rangle_{A,B}$, $|\tilde{0}_L\rangle_{A,B} = \cos\theta\,|0_L\rangle_{A,B} + \sin\theta\,|(0,2)S\rangle_{A,B}$, whereas the triplets remain in the states $|\tilde{1}_L\rangle_{A,B} = |1_L\rangle_{A,B}$; see Methods for the definition of θ. As illustrated in Fig. 2d, this produces a spin-selective charge dipole, which enables an effective dipole–dipole interaction. For small θ, the probability of populating $|(0,2)S\rangle$ is small ($\sim\sin^2\theta$); however, in the adiabatic basis, $V_{AB} = E_{cc}\sin^4\theta\ |\tilde{0}_L\rangle\langle\tilde{0}_L|_A \otimes |\tilde{0}_L\rangle\langle\tilde{0}_L|_B$, which allows for a controlled phase gate of angle π when the biasing is on for a time $\pi\hbar/E_{cc}\sin^4\theta$. As the cross-capacitance energy may be large[36] (0.1–1 meV), this time can be in sub-nanosecond timescales. In principle, exchange-based approaches are also applicable[14,15]. However, they would temporarily take the qubit out of the logical space, leading to unprotected error accumulation.

Reliable qubit transport is an essential feature of any scalable implementation of quantum computation[37,38]. Low-error transport is difficult to achieve through pairwise SWAP gates. In our approach, we transport spin states by moving the electron charge, as described in Fig. 3. Early experiments demonstrated coherent spin transport in bulk GaAs (ref. 39); we use a deterministic transport mechanism here, greatly reducing charge-related errors. Essentially, a travelling wave potential for quantum dots is produced by modulation of fixed depletion gates. Many electrons may be carried in separate, adjacent minima, allowing parallel movement of all of the physical bits encoding a logical bit and leading to efficient blockwise two-qubit operations. With high barriers between adjacent minima, such a shuttle forms a series of unconnected quantum dots each moving with a constant velocity v. Adiabatic transport is achieved if $|v|^2 m^*/2 \ll \alpha$, where m^* is the effective mass of the electron and α is the orbital-level spacing of the moving dot, implying $|v| \ll 10^4$ m s^{-1} for an orbital-level spacing of 0.5 meV. For example, with a feature size of 50 nm, one cycle of the shuttle yields a distance of 300 nm and is adiabatic for cycle periods $\tau \sim 1$ ns.

ERRORS IN QUANTUM OPERATIONS

We now consider sources of error. The temperature must be sufficiently low for efficient preparation of singlet states in a single quantum dot, requiring $T \ll J_d/k_B \sim 5$ K, where J_d is the single-dot exchange energy and k_B the Boltzmann constant. In

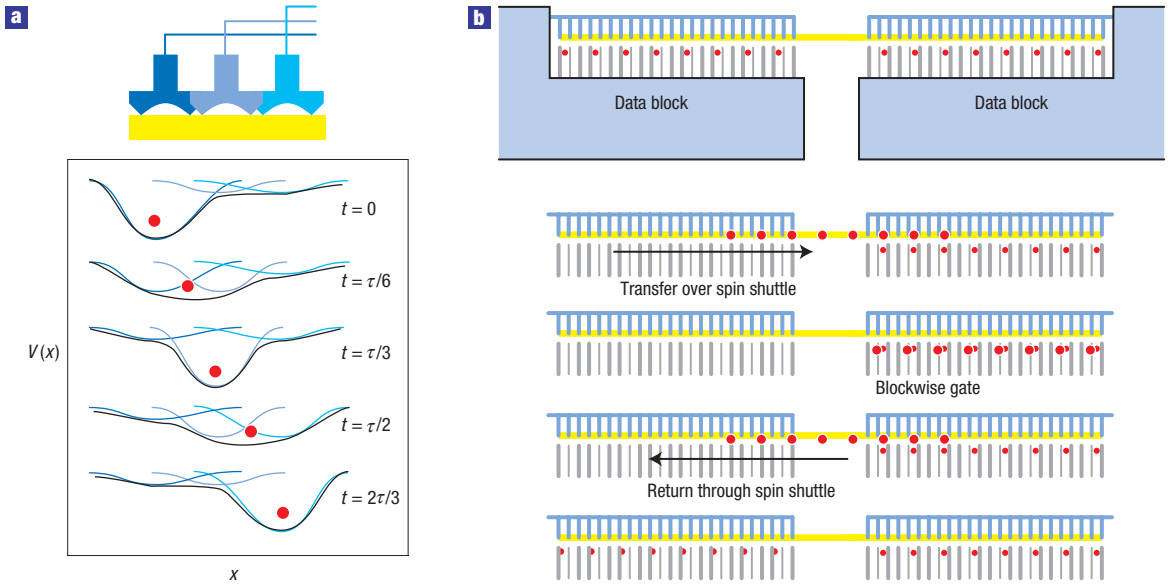

Figure 3 Long-range qubit transport. a, A single-electron charge-coupled device or electron pump[28] operates by applying a.c. varying voltages to three sets of gates $\pm 2\pi/3$ out of phase. The sign determines the direction of travel. Electrons are injected into/ejected from the transport channel by means of adiabatic pulses applied before starting or stopping motion. A gate design for the spin 'shuttle' (top) and potential energies along the transport direction at five points in time are shown at the bottom. The black curve is the total potential the electron encounters, given as the sum of the three blue curves. **b**, Many electrons may be carried in separate, adjacent minima, allowing parallel movement of all of the physical bits encoding a logical bit and leading to efficient blockwise two-qubit operations.

this regime, the dominant errors are low-frequency (spin) phase noise due to hyperfine coupling[9,18] and charge-based dephasing and relaxation. The spin noise is modelled as a time (t) and position (x) dependent term $\eta(t,x)$ interacting via $V = \hbar\eta(t,x)\hat{S}_z$, where $\eta(t,x)$ is independent for each dot, corresponding to statistically independent noise terms with weight $S(\omega)$ at frequency ω, and $\hat{S}_z$ is the electron spin projection on the external field. The spin phase noise power spectrum due to nuclei is characterized by a time-ensemble-averaged dephasing time $T_2^* \approx 10$ ns and a high-frequency cutoff $\gamma \ll 1/T_2^*$ (refs 9,17,21–23). In this error model, nuclear spin-related dephasing can be refocused with periodic Z rotations to produce a long-lived quantum memory with potential lifetimes expected to exceed milliseconds[17].

Errors incurred during Z rotations arise from charge-based dephasing because of both gate voltage fluctuations and intrinsic coupling to environmental degrees of freedom such as phonons[40–42]. We choose a noise model for charge dephasing where the rate for inelastic transitions from (0,2) to (1,1) is given by T_1^{-1} and where the energy difference Δ fluctuates, inducing characteristic charge dephasing with a rate T_2^{-1}. After elimination of the (0,2) state (see Methods) the effective error rate during an exchange gate is given by $\sin^2(\theta)T_1^{-1}[1+\sin^2(\theta)(T_1/T_2)]$, whereas the exchange energy is $J = T\tan(\theta)/2$. In principle, the error vanishes for $\theta \to 0$; however, in practice, we require that $J \gg 1/T_2^*$ owing to the spin phase noise. As an example, taking $T_1 = 3$ ns, $T_2 = 1$ ns and tunnel coupling $T = 120\,\mu$eV, $\theta \approx 0.06\pi$ is optimal with an error per SWAP of about 3×10^{-3}.

Charge noise can be further reduced by working at points where the response of the exchange energy to gate voltages is zero, that is, $\mathrm{d}J/\mathrm{d}V_i = 0$ for all gate voltages $\{V_i\}$, in analogy to such zero-derivative points in superconductor-based qubit designs[43]. Although this is true for $J = 0$, this could also be achieved for finite J if sufficient perpendicular field is applied to change the sign of J while in the separated configuration and while maintaining the singlet as the ground state of the biased configuration[44] (also M. Stopa, private communication). This naturally leads to an extremum for $J(\{V_i\})$ associated with a maximally negative J value. Only intrinsic errors and higher-order processes are not suppressed by these techniques. Finally, a Landau–Zener excitation to $|(0,2)S\rangle$ is suppressed by an energy gap of the order of the orbital-level spacing. We may neglect it in a low-temperature approximation, which is justified in our regime as no phonons of 1 meV are available in the environment to drive the inelastic transition, and if gate control is adiabatic with respect to the orbital-level spacing.

For X rotations, composite pulses allow high-fidelity operations even in the presence of substantial low-frequency (spin) phase noise. For example, the slowly varying nuclear field leads to correlated under/over rotation errors. The BB1 composite pulse sequence from NMR is effective in eliminating these errors[45]: for an under/over rotation angle $\delta\phi = \phi\hbar/T_2^*\epsilon_{dB}$, X rotation has an error $p_1 \propto \delta\phi^{-6}$. Errors due to the drift of the nuclear field over the timescale of the BB1 composite pulse can be calculated as a shift occurring over a time τ_c and enters as $p_1' = (\tau_c\epsilon_{dB})^{-1}\delta\phi^{-4}$. As a concrete example, we now consider an X rotation of $\pi/2$. Setting $U = R_X^{\pi/4}$, the required sequence is $R_{x,BB1}^{\pi/2} = UR_Z^{-\phi}U^4R_Z^{-2\phi}U^8R_Z^{2\phi}U^4R_Z^{\phi}U$ with $\phi = \cos^{-1}(-1/8)$. For a field difference between two GaAs dots of 30 mT, a spin phase noise with $T_2^* = 10$ ns and high-frequency cutoff $\gamma \leq 1\ \mu\mathrm{s}^{-1}$, the error due to under/over rotation is $p_1 \leq 10^{-4}$, the error due to drift is $p_1' \ll 10^{-4}$ and the total gate time is 3 ns. Imperfect exchange gates increase this error linearly (for small exchange errors), whereas a larger gradient reduces gate time and error. In practice, our suggested techniques for higher-fidelity exchange gates may be necessary to make composite pulses worthwhile.

Although the energy gap between singlet and triplet subspaces suppresses the spin noise during exchange gates and the two-qubit gate, charge noise becomes important owing to the finite admixture of different charge states. Taking the same charge noise model used for Z rotations, we estimate that a dephasing error during the two-qubit gate occurs with probability

$p_2 = (\pi\hbar/E_{cc})(1/T_2 + 1/T_1 \sin^2\theta)$. With $E_{cc} = 1$ meV and taking $\theta = 0.1\pi$, the error is $p_2 \leq 6 \times 10^{-3}$. Improved charge dephasing terms would lead to substantially improved operation.

During the transport process, motional averaging reduces the error due to low-frequency phase noise. The error is reduced further for our encoded qubits; by transporting individual spins of a qubit in close proximity, the encoded qubit is immune to most dephasing, as we analysed in detail[17]. Qualitatively, as the two spins of the qubit travel through the same channel, all static phase terms (including spin–orbit interaction) are cancelled exactly. Focusing on a specific case, for hyperfine terms in GaAs, with $T_2^* \sim 10$ ns, $\gamma \leq 1\ \mu s^{-1}$ and average dot-to-dot time of 1 ns, we find $T_{2,\mathrm{eff}}^* \gg 1$ ms. The spin shuttle error per dot-to-dot transfer, $p_t \simeq 10^{-6}$, is likely to be limited by the Zeeman-suppressed spin-flip terms. We note that transport over 100 sites will have higher fidelity than a single two-qubit gate.

FAULT TOLERANCE AND ERROR THRESHOLDS

The physical qubits discussed above are used to encode and protect logical computations of a quantum computer by using QEC[37,38]. We adopt an approach in which most QEC operations are performed on ancillary qubits, allowing verification of successful preparation, before interacting with qubits used for the logical computation for error correction[30]. This prevents errors occurring in the bulk of the QEC operations from affecting the logical operation. To facilitate parallel preparation and verification of ancillae, qubits are grouped into independent blocks, comprising N_b qubits, as shown in Fig. 1b. N_b is the number of qubits required to implement logical ancilla creation and verification for a given quantum-error-correcting code. For example, the Steane [[7,1,3]] code typically has $N_b \geq 10$, where the value depends on choice of verification circuitry, which could be optimized for a given error model. Blocks of R ancillae and a data block are grouped into units for a hierarchical architecture illustrated in Fig. 1.

Some errors, such as spin flips, make qubits leave the logical subspace. These leakage errors must be corrected. In addition to standard QEC[30], which only corrects within the logical subspace, at the lowest level of encoding we introduce a 'T' gate network to detect leakage errors, that is, spin flips, and replace them with errors within the logical subspace. As our two-qubit gate is insensitive to which triplet state the system is in, checking the parity of the qubit under a logical bit flip, $X = R_X^{\pi}$, detects leakage to $|\uparrow\uparrow\rangle, |\downarrow\downarrow\rangle$. More specifically, preparing an ancilla (A) in $|0_L\rangle$, the T network on a data bit (D) and ancilla is the sequence $H_A X_D {}^{C}Z_{AD} X_D {}^{C}Z_{AD} H_A$. Here H_A is a hadamard on the ancilla qubit and ${}^{C}Z_{AD}$ is a controlled phase between A and D. Then, the ancilla is measured in the Z basis; the result 1 indicates no leakage error and computation proceeds. The result 0 indicates leakage, and we replace the data qubit with the state $|0_L\rangle$. This maps errors outside the logical space to errors within the logical space and allows the normal circuitry of error correction to proceed within the logical subspace. As each qubit of the encoded qubit is operated on with independent ancilla qubits, the procedure is fault tolerant.

Finally, for scalable architectures, teleportation-based gates may be used[46,47]. Specifically, high-fidelity prior entanglement and measurement provide an alternative to the CPHASE two-qubit gate that may be appropriate for higher-level encoding and/or fault-tolerant gate operations where large transport distances or long times between gates are common. Such entangled states may be prepared using a charge measurement on spins belonging to different qubits and their fidelity may be improved by entanglement purification[17].

We now consider teleportation-based gates in more detail. By preparing entanglement in ancillary qubits in advance, Bell measurements are used to teleport the data through the gate, yielding the desired logical operation[46]. In addition, teleportation-based gates allow for the correction of arbitrary leakage errors such as electron loss and spin flips, because the data qubit is replaced with the new ancillary qubit.

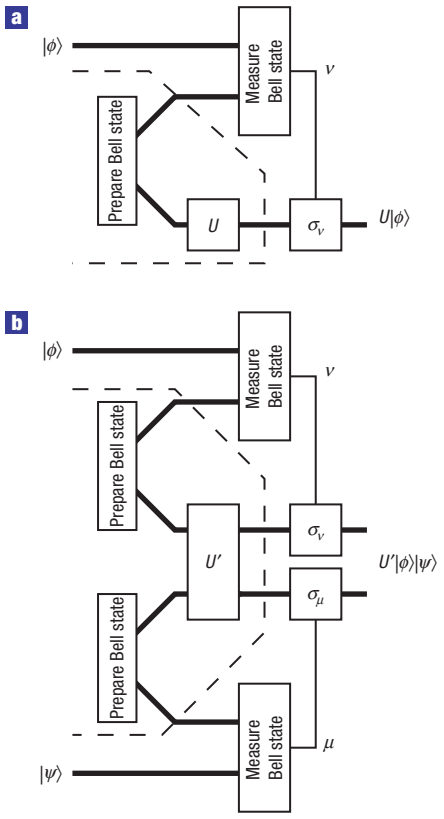

Figure 4 Teleportation-based gates. a, Teleportation-based single-qubit gates and **b**, two-qubit gates. The desired operation (U or U') is teleported onto the remaining qubit(s), with a further known Pauli operator(s) applied to the result. These Pauli operators are, as shown, **a**, σ_ν and **b**, $\sigma_\nu\sigma_\mu$.

Teleportation-based single-qubit gates and two-qubit gates start with a prepared, ancilla state with the desired unitary operation already applied to one qubit of a Bell pair, and are completed by Bell measurements on the the other qubit of the pair and the data qubit (Fig. 4). This teleports the desired operation onto the remaining qubit, with a further known Pauli operator applied to the result. These Pauli operators may be undone, as shown in Fig. 4a with σ_ν and Fig. 4b with $\sigma_\nu\sigma_\mu$. Thus, the operation of a given gate can be reduced to the preparation of a known, entangled state of ancillas (occurring inside the dashed lines), followed by Bell measurements.

The power of this teleportation technique derives from the ability to make the difficulty of gates a state-preparation problem (where states may be prepared in a probabilistic manner, for example using measurements and without using two-qubit gates; in addition, purification techniques[17] can be used to improve fidelity), and in the ability to remove arbitrary leakage errors, such as spin flips taking the system out of the logical space or even loss of an electron, by teleporting the data to the freshly prepared ancilla qubit. It also allows a Z rotation of $\pi/8$ in a fault-tolerant manner[47], completing the set of universal, fault-tolerant gate operations. In our architecture, the preparation of states could occur in the transport channel qubit (qubit B, in Fig. 1c). However, the timescale and overhead in ancilla number for such gates may

make teleportation-based leakage correction less efficient than the T network.

Detailed analysis has shown that thresholds for fault tolerance depend sensitively on the fidelity of quantum memory, quantum gate operations and errors associated with long-range qubit coupling[24,30]. With the quantum memory provided from refocusing of the logical qubit states and the transport mechanism described above, we now analyse the error requirements for reaching the fault-tolerant threshold by direct analogy to ion-trap-based schemes[24]. In both cases, transporting quantum information has low error rates, measuring quantum states takes many time steps and two-qubit gates are slower than one-qubit gates. If two-qubit gates have an error probability p_2, we can rate the overall system as follows. For one-qubit gates, the error is $p_1 < p_2$; for transport $p_t \ll p_2$. Memory error rates at critical times (such as during measurement) are $p_m \sim p_1$ owing to the use of one-qubit gates to implement dynamical protection. Transport within a block produces errors in memory and transport similar to those of a single two-qubit gate. This is analogous to the situation of ref. 24 where a threshold was numerically estimated for the [[7,1,3]] Steane code. In particular, memory error during measurement is less than two-qubit gate errors and transport of distances up to RN_b occurs with negligible overhead, giving the ultimate threshold for two-qubit gates of $p_2 \simeq 2 \times 10^{-4}$. Note that this estimate assumes that classical, local information processing requires only a few time steps of the quantum computer. Given our expected error rates, achieving fault tolerance will require error-reducing approaches, such as composite pulses and zero-derivative points. In addition, higher thresholds may be possible through better code choice and other optimizations[48].

OUTLOOK

We described and analysed a modular solid-state architecture, based on spin qubits in double quantum dots, which can be used for scalable quantum computation. The qubits were chosen for potential long quantum memory times, and we developed a long-range, low-error transport mechanism for them. From a technical perspective, static field gradients of 100 mT μm^{-1} or more and electronic gate control at 1–10 GHz were shown to be sufficient to achieve the fault-tolerant regime. In practical terms, taking a clock speed of 1 GHz, measurement within 10 clock cycles with, for example, a radiofrequency single-electron transistor[25,26], exchange gates with less than one error per 10^4 clock cycles and our low-error single-spin transport mechanism yields fault tolerance. This result is robust to low-frequency spin phase noise corresponding to $T_2^* = 10$ clock cycles and to realistically fast charge dephasing. These parameters are consistent with the current measurements for GaAs quantum dots[9,18,34].

METHODS

ELECTRICALLY CONTROLLED QUANTUM OPERATIONS

The capacitive two-qubit gate is based on the differential charge coupling E_{cc} between two double quantum dots, A and B, of states with one electron in each quantum dot (1,1) and two electrons on one side (0,2). These correspond to the logical states and the doubly occupied singlets, $|(0,2)S\rangle_A$ and $|(0,2)S\rangle_B$, for each double dot. We choose a labelling of dots such that the second dot of A and the second dot of B are adjacent, maximizing their Coulomb interaction. The Coulomb interaction gives a charge-based interaction that has a factorizable component

$$V_A + V_B = \Delta_A(P_A^L - |(0,2)S\rangle\langle(0,2)S|_A) + \Delta_B(P_B^L - |(0,2)S\rangle\langle(0,2)S|_B),$$

and an entangling component

$$V_{AB} = E_{cc}|(0,2)S\rangle\langle(0,2)S|_A \otimes |(0,2)S\rangle\langle(0,2)S|_B,$$

where

$$P_{A(B)}^L = |0_L\rangle\langle 0_L|_{A(B)} + |1_L\rangle\langle 1_L|_{A(B)}$$

projects into the logical subspace of A(B). The residual term leads to capacitive coupling in the charge stability diagram of the combined system and is set by the device geometry. It has been observed in parallel quantum dots to be of the order of $E_{cc} = 0.1$ to 1 meV (ref. 36).

A simple form of the capacitive two qubit gate can be realized by starting in the unbiased configuration, in which the logical states are both (1,1) charge states. Then, rapid adiabatic passage to the (0,2) configuration for qubits A and B will lead to state-selective transfer: only the singlet states will go to the doubly occupied states $|(0,2)S\rangle$. The Coulomb interaction $V_A + V_B$ leads to an exchange gate for A and B, whereas V_{AB} leads to further phase evolution for the state $|(0,2)S\rangle_A|(0,2)S\rangle_B$. By waiting at time $\hbar\pi/E_{cc}$ a further π phase is accumulated for this state, realizing a controlled-phase operation and two Z rotations. The Z rotations can be undone with further, independent exchange gates performed in series on qubits A and B.

In a realistic situation, charge dephasing limits the fidelity of this gate[40,41] and the strength of the interaction makes control delicately sensitive to pulse parameters at picosecond timescales. To mitigate these factors, a partial transfer to the (0,2)S states is achieved when the system is biased only slightly. This reduces the coupling to charge-related dephasing and increases the timescale for gate operation leading to lower sensitivity to pulse parameters. For a double quantum dot with the level structure given in Fig. 2, we may eliminate the doubly occupied states when the gap Δ is much larger than manipulation frequencies. To do so, we start by writing the three-level hamiltonian for $|1_L\rangle$, $|0_L\rangle$ and $|(0,2)S\rangle$:

$$H = \begin{pmatrix} 0 & \epsilon_{dB}/2 & 0 \\ \epsilon_{dB}/2 & 0 & T \\ 0 & T & \Delta \end{pmatrix}.$$

Adiabatic elimination[49] yields an effective hamiltonian to order T/Δ for the states $|1_L\rangle$, $|\tilde{0}_L\rangle$:

$$H_{eff} = \begin{pmatrix} 0 & \epsilon_{dB}/2 \\ \epsilon_{dB}/2 & T^2/\Delta \end{pmatrix},$$

where the effective exchange energy is $J = T^2/\Delta$, as in the main text. Higher-order corrections may be kept within the logical subspace as long as manipulation times are much slower than $\hbar/\Delta$. By changing the bias parameter in each dot to be near the (1,1) to (0,2) singlet transition, the singlet state is mapped to the adiabatic ground state, $|\tilde{0}_L\rangle = \cos(\theta)\,|(1,1)S\rangle + \sin(\theta)\,|(0,2)S\rangle$, where $\theta = \arctan[(\Delta - \sqrt{\Delta^2 + 4T^2})/2T]$ is the adiabatic angle and $J = T\tan(\theta)/2$. The renormalized interaction V_{cc} becomes $E_{cc}\sin^4(\theta)|\tilde{0}_L\rangle\langle\tilde{0}_L|_A \otimes |\tilde{0}_L\rangle\langle\tilde{0}_L|_B$. Critically, the effective exchange energy between $|1_L\rangle$ and $|\tilde{0}_L\rangle$ becomes only quadratically sensitive to fluctuations of the energy differences Δ_A and Δ_B, reducing the sensitivity to charge dephasing.

Received 17 August 2005; accepted 2 November 2005; published 1 December 2005.

References

1. Loss, D. & DiVincenzo, D. Quantum computation with quantum dots. *Phys. Rev. A* **57,** 120–126 (1998).
2. Makhlin, Y., Schön, G. & Shnirman, A. Quantum-state engineering with Josephson-junction devices. *Rev. Mod. Phys.* **73,** 357–400 (2001).
3. Nakamura, Y., Pashkin, Y. & Tsai, J. Coherent control of macroscopic quantum states in a single-Cooper-pair box. *Nature* **398,** 786–788 (1999).
4. Chiaverini, J. *et al.* Implementation of the semiclassical quantum Fourier transform in a scalable system. *Science* **308,** 997–1000 (2005).
5. Cirac, J. I. & Zoller, P. New frontiers in quantum computation with atoms and ions. *Phys. Today* **57,** 38–44 (2004).
6. Chiorescu, I., Nakamura, Y., Harmans, C. & Mooij, J. Coherent quantum dynamics of a superconducting flux qubit. *Science* **299,** 1869–1871 (2003).
7. Heij, C., Dixon, D., van der Wal, C., Hadley, P. & Mooij, J. Quantum superposition of charge states on capacitively coupled superconducting islands. *Phys. Rev. B* **67,** 144512 (2003).
8. Wallraff, A. *et al.* Strong coupling of a single photon to a superconducting qubit using circuit quantum electrodynamics. *Nature* **431,** 162–167 (2004).
9. Petta, J. *et al.* Coherent manipulation of coupled electron spins in semiconductor quantum dots. *Science* **309,** 2180–2184 (2005).
10. Duan, L.-M. & Guo, G.-C. Preserving coherence in quantum computation by pairing quantum bits. *Phys. Rev. Lett.* **79,** 1953–1956 (1997).
11. Zanardi, P. & Rasetti, M. Noiseless quantum codes. *Phys. Rev. Lett.* **79,** 3306–3309 (1997).
12. Lidar, D. A., Chuang, I. L. & Whaley, K. B. Decoherence-free subspaces for quantum computation. *Phys. Rev. Lett.* **81,** 2594–2597 (1998).
13. Viola, L., Knill, E. & Lloyd, S. Dynamical generation of noiseless quantum subsystems. *Phys. Rev. Lett.* **85,** 3520–3523 (2000).
14. Wu, L.-A. & Lidar, D. A. Creating decoherence-free subspaces using strong and fast pulses. *Phys. Rev. Lett.* **88,** 207902 (2002).
15. Levy, J. Universal quantum computation with spin-1/2 pairs and Heisenberg exchange. *Phys. Rev. Lett.* **89,** 147902 (2002).
16. Mohseni, M. & Lidar, D. A. Fault-tolerant quantum computation via exchange interactions. *Phys. Rev. Lett.* **94,** 040507 (2005).
17. Taylor, J. M. *et al.* Solid-state circuit for spin entanglement generation and purification. *Phys. Rev. Lett.* **94,** 236803 (2005).

18. Johnson, A. C. *et al.* Triplet–singlet spin relaxation via nuclei in a double quantum dot. *Nature* **435,** 925–928 (2005).
19. Bracker, A. S. *et al.* Optical pumping of electronic and nuclear spin in single charge-tunable quantum dots. *Phys. Rev. Lett.* **94,** 047402 (2005).
20. Koppens, F. H. L. *et al.* Control and detection of singlet-triplet mixing in a random nuclear field. *Science* **309,** 1346–1350 (2005).
21. Merkulov, I. A., Efros, Al. L. & Rosen, M. Electron spin relaxation by nuclei in semiconductor quantum dots. *Phys. Rev. B* **65,** 205309 (2002).
22. Khaetskii, A., Loss, D. & Glazman, L. Electron spin decoherence in quantum dots due to interaction with nuclei. *Phys. Rev. Lett.* **88,** 186802 (2002).
23. de Sousa, R. & Das Sarma, S. Electron spin coherence in semiconductors: Considerations for a spin-based solid-state quantum computer architecture. *Phys. Rev. B* **67,** 033301 (2003).
24. Steane, A. M. Overhead and noise threshold of fault-tolerant quantum error correction. *Phys. Rev. A* **68,** 042322 (2003).
25. Devoret, M. H. & Schoelkopf, R. J. Amplifying quantum signals with the single-electron transistor. *Nature* **406,** 1039–1046 (2000).
26. Lu, W., Ji, Z., Pfeiffer, L., West, K. W. & Rimberg, A. J. Real-time detection of electron tunnelling in a quantum dot. *Nature* **423,** 422–425 (2003).
27. Engel, H.-A. *et al.* Measurement efficiency and n-shot readout of spin qubits. *Phys. Rev. Lett.* **93,** 106804 (2004).
28. Ono, Y., Fujiwara, A., Nishiguchi, K., Inokawa, H. & Takahashi, Y. Manipulation and detection of single electrons for future information processing. *J. Appl. Phys.* **97,** 031101 (2005).
29. Kielpinski, D., Monroe, C. & Wineland, D. Architecture for a large-scale ion-trap quantum computer. *Nature* **417,** 709–711 (2002).
30. Steane, A. M. Quantum computer architecture for fast entropy extraction. *Quant. Inf. Comput.* **2,** 297–306 (2002).
31. Svore, K. M., Terhal, B. M. & DiVincenzo, D. P. Local fault-tolerant quantum computation. *Phys. Rev. A* **72,** 022317 (2005).
32. Petta, J. R., Johnson, A. C., Marcus, C. M., Hanson, M. P. & Gossard, A. C. Manipulation of a single charge in a double quantum dot. *Phys. Rev. Lett.* **93,** 186802 (2004).
33. Khaetskii, A. V. & Nazarov, Y. V. Spin-flip transitions between Zeeman sublevels in semiconductor quantum dots. *Phys. Rev. B* **64,** 125316 (2001).
34. Hanson, R. *et al.* Zeeman energy and spin relaxation. *Phys. Rev. Lett.* **91,** 196802 (2003).
35. Monzon, F. G., Johnson, M. & Roukes, M. L. Strong Hall voltage modulation in hybrid ferromagnetic/semiconductor microstructures. *Appl. Phys. Lett.* **71,** 3087–3089 (1997).
36. van der Wiel, W. G. *et al.* Electron transport through double quantum dots. *Rev. Mod. Phys.* **75,** 1–22 (2003).
37. Shor, P. W. Scheme for reducing decoherence in quantum computer memory. *Phys. Rev. A* **52,** R2493–R2496 (1995).
38. Steane, A. M. Error correcting codes in quantum theory. *Phys. Rev. Lett.* **77,** 793–796 (1996).
39. Kikkawa, J. M. & Awschalom, D. D. Lateral drag of spin coherence in gallium arsenide. *Nature* **397,** 139–141 (1999).
40. Brandes, T. & Vorrath, T. Adiabatic transfer of electrons in coupled quantum dots. *Phys. Rev. B* **66,** 075341 (2003).
41. Barrett, S. D. & Barnes, C. H. W. Double-occupation errors induced by orbital dephasing in exchange-interaction quantum gates. *Phys. Rev. B* **66,** 125318 (2002).
42. Hu, X. & Das Sarma, S. Charge fluctuation induced dephasing of exchange coupled spin qubits. Preprint at <http://arxiv.org/abs/cond-mat/0507725> (2005).
43. Vion, D. *et al.* Manipulating the quantum state of an electrical circuit. *Science* **296,** 886–889 (2002).
44. Burkard, G., Loss, D. & DiVincenzo, D. P. Coupled quantum dots as quantum gates. *Phys. Rev. B* **59,** 2070–2078 (1999).
45. Vandersypen, L. M. & Chuang, I. L. NMR techniques for quantum control and computation. *Rev. Mod. Phys.* **76,** 1037–1069 (2004).
46. Gottesman, D. & Chuang, I. L. Demonstrating the viability of universal quantum computation using teleportation and single-qubit operations. *Nature* **402,** 390–393 (1999).
47. Zhou, X., Leung, D. W. & Chuang, I. L. Methodology for quantum logic gate constructions. *Phys. Rev. A* **62,** 052316 (2000).
48. Knill, E. Quantum computing with realistically noisy devices. *Nature* **434,** 39–44 (2005).
49. Cohen-Tannoudji, C., Dupont-Roc, J. & Grynberg, G. *Atom-Photon Interactions: Basic Processes and Applications* (Wiley, New York, 1992).

Acknowledgements

We gratefully acknowledge conversations with J. Folk, A. Houck, A. C. Johnson, D. Loss and especially J. Petta. The work at Harvard was supported by ARO/ARDA, DARPA-QuIST, NSF Career award, NSF grant DMR-02-33773, Alfred P. Sloan Foundation, and David and Lucile Packard Foundation. The work at Innsbruck was supported by the ÖAW through project APART (W.D.), the European Union and the Austrian Science Foundation.
Correspondence and requests for materials should be addressed to J.M.T.

Competing financial interests

The authors declare that they have no competing financial interests.